

Modeling flow over an initially dry bed

Modélisation de l'écoulement sur un lit initialement sec

ABDUL A. KHAN, *Research Assistant Professor, National Center for Computational Hydroscience and Engineering, The University of Mississippi, 102 Carrier Hall, University, MS 38677, The U. S. A., E-mail: akhan@ncche.olemiss.edu*

ABSTRACT

The one-dimensional groundwater flow equations are coupled with the St. Venant equations to simulate the flow resulting from a sudden removal of a dam over an initially dry downstream bed. The St. Venant equations are solved using a Petrov-Galerkin finite element scheme, while the groundwater flow equations are solved using the Bubnov-Galerkin finite element scheme. The comparison of the computed water surface and discharge per unit width profiles with the corresponding analytical solutions, for a dambreak over frictionless horizontal bed, show that the model possesses excellent phase accuracy, for both positive and negative waves, and can predict the discharge distribution accurately. Also, the computed water surface profiles are compared with the available measured data for the dambreak flows over smooth and rough surfaces of horizontal and sloping channels. In addition, the results obtained from only the St. Venant equations with minimum depth criteria are presented for comparison with the above model.

RÉSUMÉ

Les équations unidimensionnelles de l'écoulement souterrain sont couplées avec les équations de Saint-Venant pour simuler l'écoulement résultant de l'effacement instantané d'un barrage sur un lit aval initialement sec. Les équations de Saint-Venant sont résolues à l'aide d'un schéma d'éléments finis de Petrov-Galerkin alors que celles relatives à l'écoulement souterrain sont résolues par un schéma d'éléments finis de Bubnov-Galerkin. La comparaison des lignes d'eau et des débits unitaires avec les solutions analytiques correspondantes, pour une rupture de barrage sur lit horizontal sans frottement, montre que le modèle numérique présente une excellente précision en phase, tant pour une onde positive que pour une onde négative, et qu'il peut prédire la distribution des débits également avec précision. Les lignes d'eau calculées ont aussi été comparées avec des mesures disponibles sur lit lisse ou rugueux, horizontal ou incliné. Par ailleurs, des résultats obtenus à partir des seules équations de Saint-Venant avec un critère de profondeur minimum, sont présentés pour comparaison avec le modèle décrit auparavant.

Introduction

The study of open channel flow over an initially dry bed is important in cases of simulating overflow of main channel flow over a dry flood plain, flow over islands during rising flood stage, flow downstream of the hydraulic structures (such as dams and gates) during intermittent release of water, and flood wave, either due to natural causes or sudden failure of a hydraulic structure, over an initially dry bed. In the literature, the flow simulation over dry channel bed has been tested traditionally by simulating the wave travelling over a dry bed after sudden removal of a dam.

In this study, the flow over an initially dry bed is simulated by coupling groundwater flow equations with the St. Venant equations following the implementation by Ghanem (1995) for the two-dimensional depth-averaged flow model. Based on the specified minimum depth criteria either St. Venant or groundwater flow equations are solved at a particular point in the flow domain. A semi-implicit finite element scheme is employed to solve either set of equations. The St. Venant equations are solved using a Petrov-Galerkin finite element scheme and the groundwater flow equations are solved using the Bubnov-Galerkin finite element scheme. The model is able to resolve the initial strong discontinuity without resort to an analytical solution for providing smoother initial conditions. In addition, the location and the profile of the surge front are obtained as parts of the solution, eliminating the need for any special treatment near the surge front. The appearance of negative depths due to numerical oscillation near the vicinity of a surge front can be handled without any special attention.

To verify the above model, three test cases are selected. First, the computed results of a dambreak surge on a frictionless hori-

zontal bed are compared to the analytical solution. Second, a dambreak experiment conducted by Schoklitsch (1917) is simulated and the results are compared with the measured data. Lastly, the measured data of water surface profiles obtained by U. S. Army Corps of Engineers (1960 and 1961), on smooth and rough beds, after an instantaneous removal of the dam are compared with the simulated results at various stations.

In addition, only the St. Venant equations are solved using a Petrov-Galerkin finite element scheme as an alternative to the above scheme. It is well known that for zero depths the St. Venant equations become numerically unstable, making it essential to check the depth at each node against specified minimum depth. If the computed flow depth, at any point in the solution domain, is smaller than the specified minimum depth, the flow depth is set to the specified minimum depth.

Equations modeled

Referring to Fig. 1, the St. Venant equations can be written as:

$$\frac{\partial h}{\partial t} + \frac{\partial q}{\partial x} = 0 \quad (1)$$

$$\frac{\partial h}{\partial t} + \frac{\partial}{\partial x} \left(\frac{q^2}{h} \right) + \frac{\partial}{\partial x} \left(\frac{gh^2}{2} \right) = gh(S_o - S_f) \quad (2)$$

where h is the water surface elevation measured from bed, q the discharge per unit width, g the gravitational acceleration, S_o the bed slope, t the time, and x the longitudinal distance. The friction slope, S_f , is evaluated as follows (van Rijn, 1993):

Revision received January, 2000. Open for discussion till April 30, 2001.

$$S_f = \frac{u|u|}{gRC_*^2}; C_* = 5.75 \log\left(\frac{R}{k}\right) + 6.2; \quad (3)$$

$$k = k_s + k_v; k_v = \frac{3.3\nu}{\sqrt{gRS_f}}$$

where R is the hydraulic radius, k_s the roughness height, k_v the viscous sub-layer thickness, ν the kinematic viscosity of the fluid, and u the longitudinal flow velocity. It should be mentioned here that, although, the depth is allowed to fall below the bed level, the St. Venant equations are applied only in the regions where depth is positive. Note that for (R/k) value of about 1/12 and smaller, C_* value becomes negative. This provides a first estimate of the minimum depth criteria, below which the groundwater flow equations should be applied.

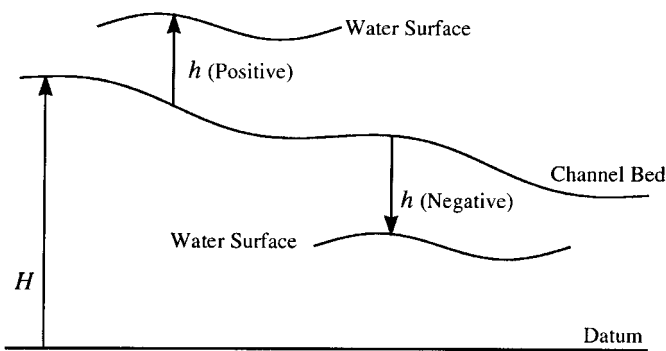


Fig. 1. Definition sketch.

The groundwater flow equations are:

$$S \frac{\partial h}{\partial t} + \frac{\partial q}{\partial x} = 0 \quad (4)$$

$$\frac{\partial h}{\partial x} + \frac{1}{T} q = S_o \quad (5)$$

where S is the storativity (and is equal to the porosity for an unconfined aquifer, i.e., ratio of volume of voids to the total volume), T the aquifer transmissivity and is equal to the product of the aquifer permeability and aquifer thickness.

As stated above, based on the specified minimum depth criteria, either St. Venant equations or groundwater flow equations are solved at a given point in the flow domain. Thus the addition of the groundwater flow equations do not present any extra computational cost. In fact, these equations are much simpler than the St. Venant equations.

In order to solve the groundwater flow equations, the values of storativity (S) and transmissivity (T) need to be specified. In cases where these equations are added only for modeling surface water flow over a dry bed, the values of S and T should be selected so as to minimize the groundwater flow. The ground-

water flow equations, for constant bed slope and transmissivity, can be written as:

$$\frac{\partial h}{\partial t} = \frac{T}{S} \frac{\partial^2 h}{\partial x^2} = D \frac{\partial^2 h}{\partial x^2} \quad (6)$$

which represents an unsteady diffusion equation. The diffusion coefficient (D) is the ratio of transmissivity and storativity. In order to minimize the groundwater flow the parameter S should be large (not greater than unity), while T should be small. For the present study, the value of storativity is fixed at unity.

Numerical scheme

The groundwater flow equations, representing unsteady diffusion equations, do not require any special numerical treatment and are solved using Bubnov-Galerkin finite element scheme (see, for example, Burnett 1987). The St. Venant equations are solved using a Petrov-Galerkin scheme. The equations are upwinded using the Characteristic Dissipative Galerkin Scheme of Hicks and Steffler (1992). The scheme provides selective dissipation for shock capturing. The optimal value of the upwinding parameter, based on the linear Fourier analysis, was found to be 0.5 and is used for all the test cases. In addition, the Courant number (given by $u\Delta t/\Delta x$; where Δx is the spatial discretization, Δt the time step, and u the wave speed) of about 0.5 was suggested by the above authors to balance space and time errors and is adopted in this study.

The system of equations, whether St. Venant or groundwater flow equations, are discretized using linear interpolating functions, and the time derivatives are approximated using finite difference formulation. The resulting discretized set of nonlinear equations is solved semi-implicitly (implicitness factor, $\theta = 0.5$) using the Newton-Raphson iterative scheme with an analytical Jacobian. The convergence of the solution to a new time level is assessed based on the criteria outlined by Khan and Steffler (1996).

The integration over the whole domain is carried out element by element, and the global coordinates are transformed into local coordinates. The integration over each element, with limits from -1 to $+1$, is performed numerically using three-point Gaussian quadrature. At each Gauss point the depth is compared to the minimum specified depth (h_m), if the depth is less than h_m the groundwater flow equations are applied, otherwise the solution continues with the St. Venant equations.

Initial and boundary conditions

For all the tests conducted in this study, initial conditions of given water depth and zero discharge are specified upstream of the dam, while zero depth and discharge are specified downstream of the dam. A zero mass flux boundary (i.e., zero discharge) is specified at the upstream end, while no boundary condition is specified at the downstream end.

Applications of the model

Comparison with an analytical solution

The analytical solution (also known as Ritter solution) for a frictionless horizontal channel, following Henderson (1966), is given by the following equations:

$$u = \frac{2}{3} \left(\frac{X}{t} + c_o \right); \quad c_o = \sqrt{gh_o} \quad (7)$$

$$c = \frac{1}{3} \left(2c_o - \frac{X}{t} \right); \quad c = \sqrt{gh} \quad (8)$$

where h_o is the initial depth upstream of the dam and X the horizontal distance with origin at the dam. At any given time, (8) gives a parabolic water surface profile between the positive and negative wave location.

In this test, the simulated results for a dambreak on a frictionless horizontal bed are compared with the analytical solution. The initial depth upstream of the dam is set at 10 m with zero depth downstream of the dam. The channel is 2000 m long with the dam located at the middle of the channel. For all of the simulations conducted for this test case, the Courant number based on the positive wave speed is about 0.5, the domain is divided uniformly into 160 elements (12.5 m element length) and the time step is about 0.3 second.

In addition to comparing the computed results with the analytical solution, the aim of this test is to gain an insight into the selection of transmissivity, T , and minimum depth criteria, h_m . The value of storativity as mentioned above is fixed at unity. In general, if the main aim is to model surface flows only, the value of h_m and T should be as small as possible. However, the stability of the scheme may impose limit on the selection of these parameters.

To assess the influence of h_m and T on the solution, and gain an insight into the selection of these values, simulations were carried out by assigning a range of values to one of the above parameters while holding the other constant. Fig. 2 shows the computed water surface profile after 40 seconds of the removal of the dam, the h_m value is fixed at 0.1 percent of the initial depth upstream of the dam, and the value of transmissivity ranges from 1.0 to 0.01 m²/s. The solution is relatively insensitive to the value of the transmissivity, except for very small value of 0.01 m²/s. The sudden change in discharge, due to the application of groundwater flow equations below h_m , causes a small undulation in the water surface profile near the tip of the wave, and for transmissivity value of 0.01 m²/s the undulation starts to grow. Although, for modeling surface flows, the value of transmissivity should be as small as possible, a very small value may cause a sharp peak near the tip of the surge. However, considering the insensitivity of the results for a wide range of values, a value of 0.1 m²/s is adequate. It should be mentioned here that for the same values of h_m and T , better results were obtained for finer discretization.

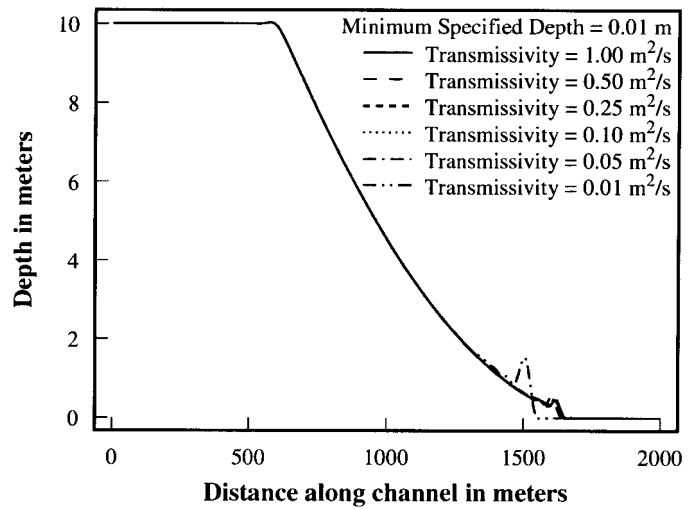


Fig. 2. Effect of the value of transmissivity (At 40 seconds after the removal of the dam).

Fig. 3 is similar to the previous figure, except the value of transmissivity is fixed at 0.1 m²/s and the value of h_m is varied from 0.1 m to 0.001 m. The computed water surface profiles are more sensitive to the value of h_m , and the shape of the surge front approaches to that predicted by the analytical solution as the value of h_m is reduced. The best results are obtained for h_m of 0.001 m (0.01 percent of the initial depth upstream of the dam). The computed specific discharge profile follows the same trend for both parameters.

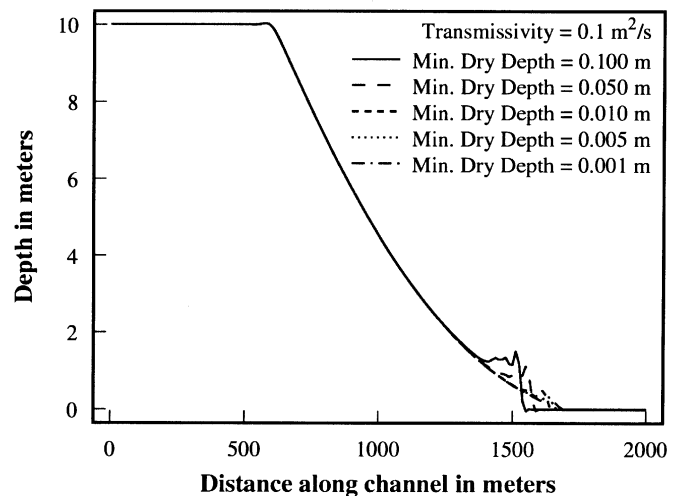


Fig. 3. Effect of the value of minimum dry depth (At 40 seconds after the removal of the dam).

Fig. 4 shows the comparison of the water surface profile obtained from the above model with that of analytical solution. For this test, the minimum specified depth h_m , below which the groundwater flow equations are used, is set to 1 mm and the transmissivity is set to 0.1 m²/s. In addition, the results obtained using only the St. Venant equations are also shown. The numerical solution in this case could not be obtained for h_m below 5 cm. In case of the St. Venant equations only, the results show that suppressing the oscillations immediately downstream of the surge, by not allowing the depth to fall below 5 cm has an

adverse effect on the solution upstream of the surge. Also, the results show poor phase accuracy. The coupling of groundwater flow equations result in a highly improved solution, the oscillation near the tip of the wave and the existence of negative depths do not cause the solution to deteriorate. The water surface profile follows the analytical solution closely with excellent phase accuracy both for positive and negative wave. The latter is an attribute of the Characteristic Dissipative Galerkin Scheme and is preserved by coupling the groundwater flow equations with the St. Venant equations.

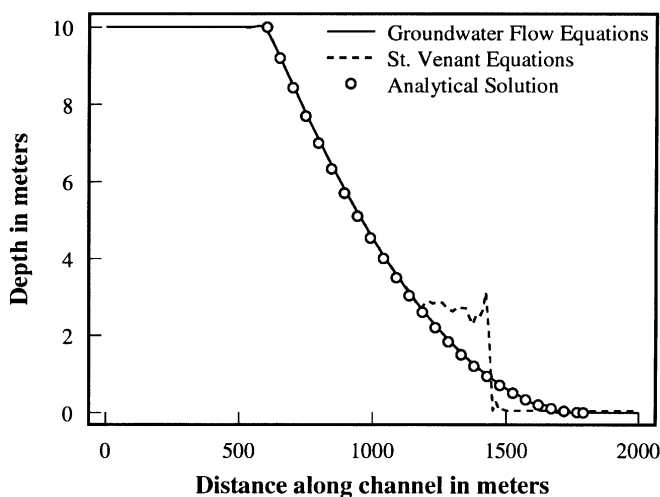


Fig. 4. Water surface profiles for frictionless horizontal bed (At 40 seconds after the removal of the dam).

Fig. 5 shows a comparison of the discharge per unit width computed using the above model and that obtained from analytical solution using (7) and (8). An excellent match shows that the mass conservation characteristic of the numerical scheme is preserved using the groundwater flow equations. The peak discharge is simulated accurately, however, near the tip of the surge the specific discharge profile deviates slightly from the analytical solution and matches exactly with the undulation in the water surface profile.

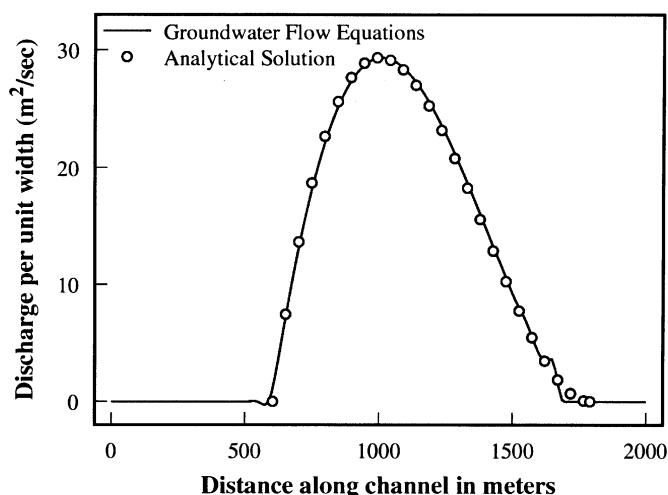


Fig. 5. Discharge profiles for frictionless horizontal bed (At 40 seconds after the removal of the dam).

Comparison with the measured data

Schoklitsch (1917) measured water surface profiles at different times after instantaneous removal of a dam located in the middle of a horizontal flume. The flume, made of smoothed wood, was 0.096 m wide and 0.08 m high. The water was ponded to a height of 0.074 m with a dry bed downstream of the dam. The numerical simulation is performed using uniform spatial discretization 0.1 m and time step size of 0.05 seconds. The Courant number based on the positive wave speed is about 0.5. The transmissivity is set to 0.01 m²/s and h_m is set at 0.5 mm. For the roughness height of smooth wood Streeter and Wylie (1981) suggested a value in the range of 0.18 mm to 0.9 mm. For the numerical simulation a value of 0.5 mm is used.

Fig. 6 shows the computed water surface profiles along with the measured data at 3.75 seconds and 9.40 seconds after the removal of the dam. The present model is capable of simulating accurately the water surface profiles. Small numerical oscillations appearing with small negative depths do not deteriorate the solution and are simply modeled as groundwater flow.

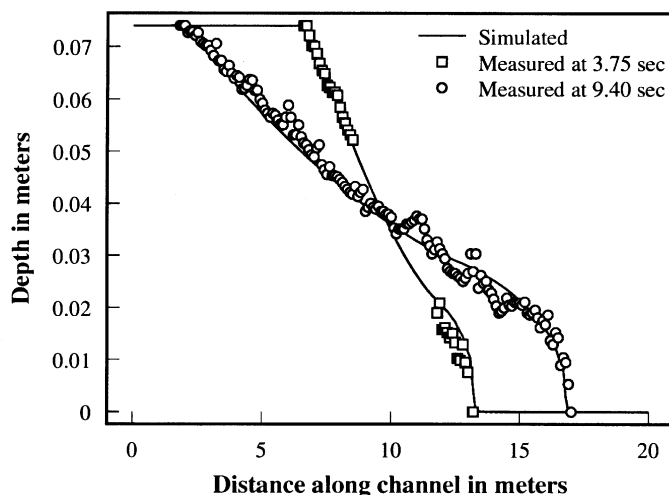


Fig. 6. Water surface profiles for smooth horizontal bed.

A series of dambreak experiments were conducted at the Waterways Experiment Station (WES) by U. S. Army Corps of Engineers (1960 and 1961). The test flume was 121.92 m (400 ft) long horizontally and was set on a slope of 0.005 (i.e., 1 foot per 200 feet horizontally). The dam was located at the midsection and water was ponded to a depth of 0.3048 m (1 ft), immediately upstream of the dam, thus having a zero depth at the upstream end of the flume. Two sets of experiment were performed and were labeled as “conditions of minimum resistance” and “condition of high resistance”. For the first case the flume was lined with plastic coated plywood, the value of Manning’s coefficient was found to be 0.009, however, variation with the depth of flow was noticed. A value of 0.05 mm for k_s , predicted accurately the arrival of the wave at the farthest station downstream of the dam and was determined by trial and error. For a depth of 0.15 m (0.5 ft), the value of Manning’s n , obtained by equating the discharge using Manning’s equation and (3), is 0.0088 and corresponds well to the suggested value.

The bed in the second case was made rough by fixing 1.9 cm by 1.9 cm (3/4 inch by 3/4 inch) aluminum angles to the floor and sides of the flume at 0.1524 m (6 inches) interval. The Manning's coefficient was found to vary from 0.15 to 0.04 for the variation of normal depth between 3 cm to 19 cm. A value of 15 cm for k_s , determined as discussed above, is used for the rough bed case. The corresponding value of Manning's n for a depth of 0.15 m (0.5 ft) is 0.04 and corresponds well to the value of the Manning's coefficient provided in the above report. The two cases, discussed above, are simulated by dividing the channel uniformly into 400 elements. The time step size is 0.08 second for the smooth bed and 0.23 second for the rough bed. The Courant number based on the speed of the positive wave is about 0.5 for both cases. The value of transmissivity is $0.0001 \text{ m}^2/\text{s}$ for both smooth and rough bed, h_m is 0.3 mm for the smooth bed and for the rough bed a value of 1.9 cm based on the physical constraint is adopted.

Figs. 7 and 8 show the computed and measured water surface profiles at four different stations for smooth bed condition. Fig. 7 shows the water surface profiles at 39.62 m and 5.79 m (130 ft and 19 ft) upstream of the dam. Both the arrival time of negative wave and water surface elevation are accurately predicted. The exposition of the bed with time in the region upstream of the dam can be modeled without difficulty. Fig. 8 shows the computed and measured water surface profiles at 7.62 m and 45.72 m (25 ft and 150 ft) downstream of the dam. Both the arrival time of positive wave and water surface elevation are predicted accurately.

Figs. 9 and 10 show the computed and measured water surface profiles at four different locations for rough bed case. Fig. 9 shows the water surface profiles at 39.62 m and 6.10 m (130 ft and 20 ft) upstream of the dam, while Fig. 10 shows the water surface profiles at 7.62 m and 45.72 m (25 ft and 150 ft) downstream of the dam. The model predicts well the arrival time for positive and negative waves and water surface elevation both upstream and downstream of the dam for high hydraulic resistance.

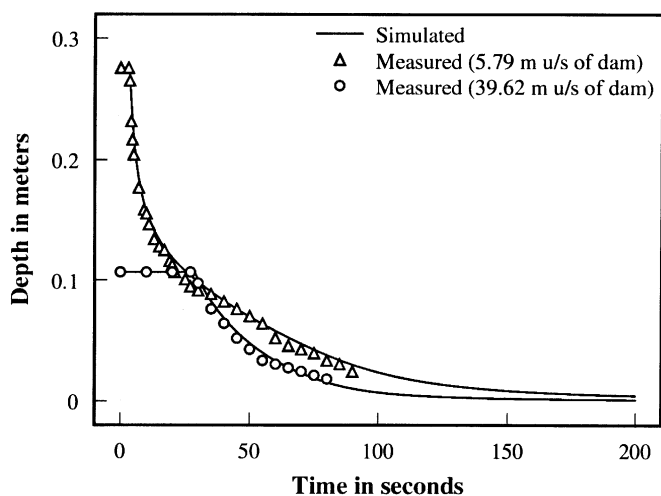


Fig. 7. Water surface profiles for smooth sloping bed.

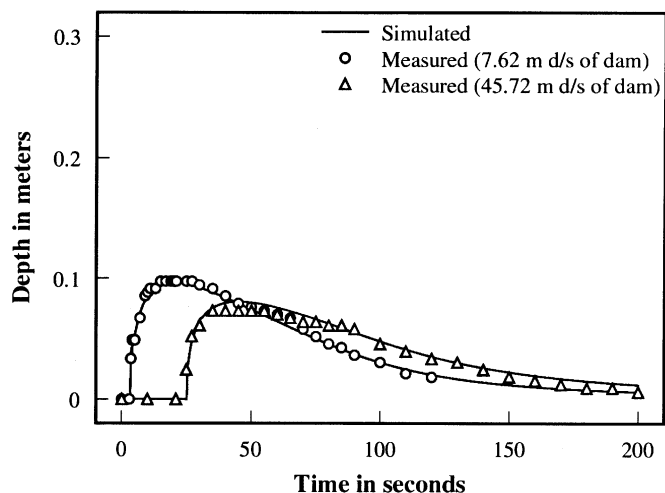


Fig. 8. Water surface profiles for smooth sloping bed.

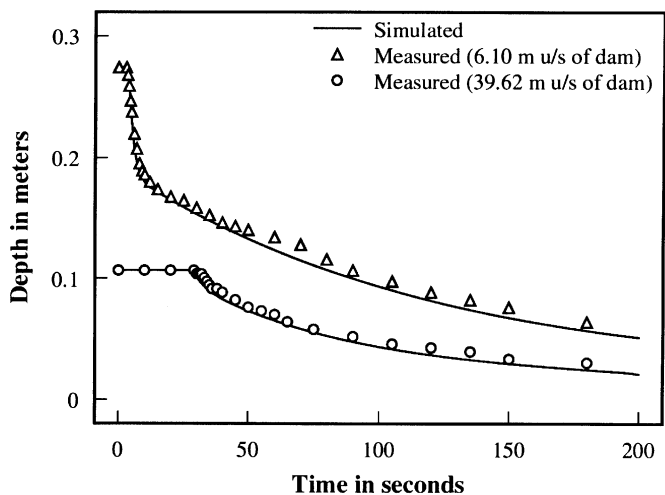


Fig. 9. Water surface profiles for rough sloping bed.

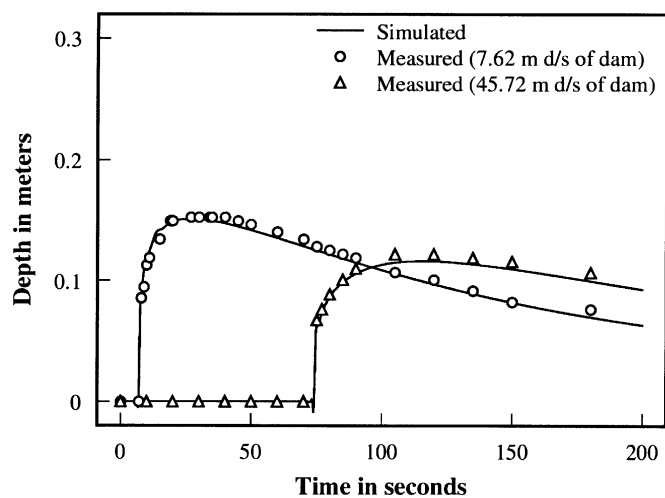


Fig. 10. Water surface profiles for rough sloping bed.

Summary and conclusions

In this study, the flow over initially dry bed is simulated by coupling groundwater flow equations with the St. Venant equations. Based on the specified minimum depth criteria either the St. Venant equations or groundwater flow equations are applied.

The above model is verified by comparing the computed results with analytical solution and measured data. As a first test, the computed water surface elevation and discharge per unit width for a dambreak wave over a frictionless horizontal channel, with dry bed downstream of the dam, is compared with the analytical solution. The computed water surface elevation together with the speed of positive and negative waves agree well with the analytical solution. The computed and analytical discharges per unit width show good agreement. Two more tests of dambreak over initially dry bed downstream of the dam are performed: the second test is for a smooth horizontal bed; and the third test, consisting of two cases, is for sloping channel with smooth and rough bed. The computed water surface profiles agree well with the measured data in each case.

The tests conducted in this study show that the above model is able to resolve the strong initial discontinuity and does not require any special treatment near the surge front. The small negative depths occurring at the front of the surge due to numerical oscillations do not pose any problem. Simulation of dambreak using St. Venant equations with minimum depth criteria shows that the removal of these oscillations near the surge front may deteriorate the solution.

Notations

c	celerity of the shallow water gravity wave;
c_o	celerity based on the depth upstream of the dam;
D	diffusion coefficient;
g	acceleration due to gravity;
h	depth of flow;
h_m	minimum specified depth;
h_o	initial depth upstream of the dam;
k_s	roughness height;
k_v	viscous sublayer thickness;
q	discharge per unit width of channel;
R	hydraulic radius;
S	storativity of the aquifer;
S_f	friction slope;
S_o	bed slope;
T	transmissivity of the aquifer;
t	time;
u	longitudinal velocity;
X	horizontal distance with origin at the dam;
x	coordinate in horizontal direction;
Δx	spatial discretization;
Δt	time step;
θ	implicitness factor; and
ν	kinematic viscosity of the fluid.

References

- BURNETT, D.S. (1987). "Finite Element Analysis." Addison-Wesley Publishing Company, pp 844.
- GHANEM, A.H. (1995). "Two-Dimensional Finite Element Modeling of Flow in Aquatic Habitats." Ph.D. thesis, University of Alberta, Alberta, Canada.
- HENDERSON, F.M. (1966). "Open Channel Flow." McGraw Hill Publishing, New York.
- HICKS, F.E., and STEFFLER, P.M. (1992). "Characteristic Dissipative Galerkin Scheme for open-channel flow." J. Hydr. Engrg., ADCE, 98(2), 337-352.
- KHAN, A. A., and STEFFLER, P. M. (1996). "Physically based hydraulic jump model for depth-averaged computations." J. Hydr. Engrg., ASCE, 122(10), 540-548.
- SCHOKLITSCH, A. (1917). "Ueber Dammbrechwellen." Sitzungsberichte der Kaiserlichen Akademie Wissenschaften, Viennal, Vol. 126, 1489-1514.
- STREETER, V. L., and WYLIE, E. B. (1981). "Fluid Mechanics." McGraw Hill Ryerson Limited.
- U.S. Army Corps of Engineers (1960). "Floods resulting from suddenly breached dams." Misc. Paper No. 2-374, Report 1: Conditions of Minimum Resistance. Waterways Experiment Station, Vicksburg, Mississippi.
- U.S. Army Corps of Engineers (1961). "Floods resulting from suddenly breached dams." Misc. Paper No. 2-374, Report 2: Conditions of High Resistance. Waterways Experiment Station, Vicksburg, Mississippi.
- VAN RIJN, L. C. (1993). "Principles of Sediment Transport in Rivers, Estuaries and Coastal Seas." Aqua Publications, Amsterdam, Netherlands.